J. Fluid Mech. (1991), *vol.* 229, *pp.* 531–554
Printed in Great Britain

Nonlinear waves on the surface of a falling liquid film. Part 1. Waves of the first family and their stability

By YU. YA. TRIFONOV AND O. YU. TSVELODUB
Institute of Thermophysics, Siberian Branch of USSR Academy of Sciences, Novosibirsk 630090, USSR

(Received 19 February 1990 and in revised form 31 July 1990)

The paper is devoted to a theoretical analysis of nonlinear two-dimensional waves on the surface of a liquid film freely falling down a vertical plate. Using a model system of equations, steady-state travelling periodical wave regimes have been found numerically. It is shown that some of them agree quantitatively with experimental results. The question of the stability of various wave regimes with respect to two-dimensional infinitesimal disturbances is examined. The most-amplified disturbances are evaluated.

1. Introduction

It was found experimentally by Kapitza & Kapitza (1949) that the flow of a thin viscous liquid layer is laminar for $Re < 400$–500, but the free surface, as a rule, is wavy. The flow can be divided into three sections: (i) an input section with a smooth free surface, (ii) a section of two-dimensional quasi-steady-state waves and (iii) a final section where the film flow becomes three-dimensional (see Nakoryakov, Pokusaev & Alekseenko (1981); Alekseenko, Nakoryakov & Pokusaev (1985)).

At present there are a great number of studies of the hydrodynamics of a wavy thin falling film in the literature. We discuss only the basic results, from our point of view, concerning the two-dimensional wave flow.

The first analytical solution for flow with a smooth free surface was received by Nusselt (1916). The profile of the longitudinal velocity in this case is a semiparabolic one, the film surface has a velocity maximum and the flow rate of liquid is proportional to the third power of the film thickness.

The first results concerning the stability of the laminar flow of a thin layer of viscous fluid with a free surface seem to have been obtained by Kapitza (1948). He has shown that if the value of the Reynolds number is higher than a critical one, a laminar-wave flow is energetically more preferable than a laminar parallel one.

Benjamin (1957) and Yih (1963) using an approximate analytical version of Orr–Sommerfeld's equation have found that film flow with a smooth free surface is unstable for any small flow rates. There are infinitesimal long-wave disturbances which exponentially amplify with time. Analogous results were obtained numerically by Krantz & Goren (1970) for the range of Reynolds numbers from 1 to 700.

The experiments carried out by Kapitza & Kapitza (1949) show that there is some critical flow rate at which waves on the liquid surface start to appear. If the flow rate is less than the critical one the wave regime does not develop, and in addition, external disturbances disappear. The Kapitza conclusion on the existence of a critical flow rate was further proved by some experimental works devoted to wave formation on the surface of a thin film (see, for example, Alekseenko *et al.* 1985).

Thus, discrepancies between the predicted and experimental data are likely to be due to a too small length of test section, the essential dependence of wave structure on liquid feed, the effect of surfactants on the flow, amongst other factors.

In their experimental investigation of nonlinear two-dimensional steady-state travelling waves, Kapitza & Kapitza (1949) used a short vertical section of a glass tube (250 mm long and 35 mm in diameter), with a film of water or alcohol falling down the outer surface of the tube. To regulate the wave regimes of the flow, the flow rate was pulsed. The wave amplitudes, velocities, lengths of waves, and thicknesses of films were measured. The regular steady-state travelling waves observed were classified by the authors as 'periodical' and 'single'. Experimental results only described for a periodical regime for $Re = 5$–20.

Further experimental results, more convenient and comprehensive for comparison with theory, were obtained by Nakoryakov *et al.* (1981) and Alekseenko *et al.* (1985). They presented amplitudes, phase velocity of waves, and mean thicknesses as functions of wavelength parameters. Conclusions on the regions of existence of regular waves were also suggested. To regulate the wave formation, the flow rate at the input section was pulsed. There were two characteristic types of wave profiles: wave form was similar to a sine one if the frequency was high, and essentially more nonlinear (an abrupt front to the wave and backflow from it) if the frequency was low.

The full problem of nonlinear film wave flow is difficult to consider theoretically, and therefore various simplified models are used, as a rule, to solve it.

Using the small long-wave parameter ϵ (ϵ is the ratio of the mean film thickness to the lengthscale of the waves in the x-direction) and the restriction $\epsilon \ll Re \lesssim 1$ the problem can be reduced to a single evolutional equation for the film thickness. In this case the solution of the Navier–Stokes equation is represented in the form of a series of ϵ. Then all the quantities one wants to define can be represented as polynomials of y with coefficients that are functions of only the thickness h and its derivatives. From this representation the kinematic condition on the film surface is used for deriving an equation for h. Benney (1966) considered the case when the surface tension was negligible and reduced the problem to a single evolutional equation. Gjevik (1970) included the effect of the surface tension and studied steady finite-amplitude periodic waves. In the case of small-amplitude nonlinear disturbances and for the Reynolds number $Re < 1$ Nepomnyashchy (1974) reduced the problem to a single equation including the simplest nonlinear quadratic term. Its solution gives two different types of waves which qualitatively agree with those observed experimentally: wave regimes similar to sinusoidal ones were found by Nepomnyashchy (1974); and a wave family whose limit is a solitary wave was found by Tsvelodub (1980). The character of the branching periodical steady-state travelling wave solutions was studied by Bunov, Demekhin & Shkadov (1984) and Tsvelodub & Trifonov (1989). It was demonstrated by Sivashinsky & Michelson (1980) that this equation had stochastic solutions.

In spite of qualitative agreement between the calculated wave form and the experimental one the quantitative comparison is not satisfactory. In the experiments waves were observed for moderate Reynolds number and their amplitude was of the same order as the value of mean film thickness. Therefore, it is necessary to take into account nonlinear terms of order higher than quadratic.

Kapitza (1948) suggested using the integral method to study the problem of two-dimensional wave film flow at moderate Reynolds numbers. He used the similarity of the longitudinal velocity profile and considered only long-wave disturbances. However, when deriving the model system, he mistakenly omitted some terms, the values of which were the same as those taken into account. Shkadov (1967) derived this system correctly. There is a great number of theoretical and experimental works where the correctness of similarity of a longitudinal velocity profile assumption was evaluated. Thus, Berbente & Ruckenstein (1968), when solving the problem for weakly nonlinear steady-state waves used the long-wave assumption; however, the velocity profile was expanded in powers of y/h. Their results and the results obtained by Shkadov (1967), where an analogous problem was solved with the similarity assumption, are in good agreement.

Some results have been obtained by a direct numerical simulation of the Navier–Stokes equation for two-dimensional waves with the long-wave assumption (see Geshev & Ezdin 1985); Demekhin, Demekhin & Shkadov 1983; Bach & Viladsen 1984). They are also in qualitative agreement with the integral theory. Nakoryakov *et al.* (1977) demonstrated experimentally that the velocity profile is close to a semiparabolic one for the greater part of the wave.

Shkadov's system consists of two equations, for the instantaneous liquid flow rate and the instantaneous thickness of the film. The family of weakly nonlinear steady-state solutions of this system was obtained by Shkadov (1968), who demonstrated, for a moderate Reynolds number, that the waves of this family were unstable. The negative solitary waves of this system were numerically calculated by Shkadov (1977).

2. Governing equation

We consider a two-dimensional flow of a viscous incompressible liquid on a vertical plate. A schematic of the flow and the coordinate system are shown on figure 1. Using dimensionless variables the governing equations of the fluid motion and the boundary conditions are as follows:

$$\frac{\partial u^*}{\partial t^*}+u^*\frac{\partial u^*}{\partial x^*}+v^*\frac{\partial u^*}{\partial y^*}=-\frac{\partial p^*}{\partial x^*}+\frac{\epsilon}{Re_1}\frac{\partial^2 u^*}{\partial x^{*2}}+\frac{1}{\epsilon Re_1}\left(\frac{\partial^2 u^*}{\partial y^{*2}}+3\right), \tag{2.1a}$$

$$\epsilon^2\left(\frac{\partial v^*}{\partial t^*}+u^*\frac{\partial v^*}{\partial x^*}+v^*\frac{\partial v^*}{\partial y^*}\right)=-\frac{\partial p^*}{\partial y^*}+\frac{\epsilon}{Re_1}\left(\epsilon^2\frac{\partial^2 v^*}{\partial x^{*2}}+\frac{\partial^2 v^*}{\partial y^{*2}}\right), \tag{2.1b}$$

$$\frac{\partial u^*}{\partial x^*}+\frac{\partial v^*}{\partial y^*}=0, \tag{2.1c}$$

$$u^*=v^*=0, \quad y^*=0, \tag{2.1d, e}$$

$$p^*=p_0^*-\frac{\epsilon^2 Fi^{\frac{1}{3}}3^{\frac{1}{3}}\dfrac{\partial^2 h^*}{\partial x^{*2}}}{Re_1^{\frac{5}{3}}\left(1+\epsilon^2\left(\dfrac{\partial h^*}{\partial x^*}\right)^2\right)^{\frac{3}{2}}}+\frac{2\dfrac{\epsilon}{Re_1}\dfrac{\partial v^*}{\partial y^*}\left(1+\epsilon^2\left(\dfrac{\partial h^*}{\partial x^*}\right)^2\right)}{\left(1-\epsilon^2\left(\dfrac{\partial h^*}{\partial x^*}\right)^2\right)}, \quad y^*=h^*(x^*,t^*), \tag{2.1f}$$

$$\frac{4\epsilon^2\dfrac{\partial h^*}{\partial x^*}\dfrac{\partial v^*}{\partial y^*}}{\left(1-\epsilon^2\left(\dfrac{\partial h^*}{\partial x^*}\right)^2\right)}+\frac{\partial u^*}{\partial y^*}+\epsilon^2\frac{\partial v^*}{\partial x^*}=0, \quad y^*=h^*(x^*,t^*). \tag{2.1g}$$

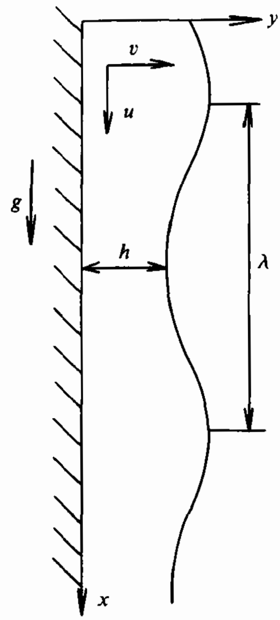

FIGURE 1. Schematic representation of a vertical falling liquid film.

Here

$$u^* = \frac{u}{u_0}, \quad v^* = \frac{v}{u_0}\frac{L}{h_0}, \quad x^* = \frac{x}{L}, \quad y^* = \frac{y}{h_0}, \quad t^* = \frac{tu_0}{L},$$

$$p^* = \frac{p}{\rho u_0^2}, \quad \epsilon = \frac{h_0}{L}, \quad Re_1 = \frac{u_0 h_0}{\nu}, \quad Fi = \frac{(\sigma/\rho)^3}{g\nu^4}, \quad u_0 = \frac{gh_0^2}{3\nu},$$

Fi is the film number, u is the velocity in the x-direction, v is the velocity in the y-direction, p is the pressure, p_0^* is the atmospheric pressure, g is the acceleration due to gravity, ν is the kinematic viscosity, ρ is the density, σ is the coefficient of surface tension, h is the instantaneous thickness of the film.

It is appropriate here to use some scale related to the wavelength L as a characteristic scale of length in the x-direction, the mean film thickness h_0 as that in the y-direction and the mean thickness velocity u_0 as a velocity scale.

Further, we shall consider only long-wave disturbances, therefore $\epsilon \ll 1$. For the range of Reynolds numbers under consideration $\epsilon \ll Re \lesssim 1/\epsilon$, after neglecting terms smaller than $O(\epsilon)$ the system (2.1) is substantially simplified. In dimensional form it is as

$$\frac{\partial u}{\partial t} + u\frac{\partial u}{\partial x} + v\frac{\partial u}{\partial y} = -\frac{1}{\rho}\frac{\partial p}{\partial x} + \nu\frac{\partial^2 u}{\partial y^2} + g, \tag{2.2a}$$

$$\frac{\partial p}{\partial y} = 0, \quad \frac{\partial u}{\partial x} + \frac{\partial v}{\partial y} = 0, \tag{2.2b, c}$$

$$p = p_0 - \sigma\frac{\partial^2 h}{\partial x^2}, \quad y = h(x,t), \tag{2.2d}$$

$$\frac{\partial u}{\partial y} = 0, \quad y = h(x,t). \tag{2.2e}$$

In addition, the following kinematic condition on the free surface must be satisfied:

$$v = \frac{\partial h}{\partial t} + u\frac{\partial h}{\partial x}, \quad y = h(x,t). \tag{2.3}$$

Deriving equations (2.2) from (2.1) we retain the term containing the capillary pressure in the boundary condition. This is possible if the film number $Fi \sim Re^5/\epsilon^6$, which is generally true for most experiments.

The system (2.2) was probably firstly derived by Levich (1959). It is easily seen that its solution is

$$v = 0, \quad u = \frac{gh_N^2}{\nu}\left(\frac{y}{h_N} - \frac{y^2}{2h_N^2}\right),$$

$$p = p_0, \quad h = h_N = \text{const}.$$

This solution is related to the Nusselt smooth flow and exists for any liquid flow rates. The other solutions of (2.2) are difficult to find. Therefore, to simplify this problem it is convenient to use the assumption self-similarity of the velocity profile:

$$u(y,x,t) = V(x,t)\,(y/h(x,t) - y^2/2h^2(x,t)). \tag{2.4}$$

For long waves this assumption is reasonable enough, but it is extremely difficult to evaluate its correctness mathematically. However, the experimental results and some direct numerical simulations show that this assumption is valid for the values of Reynolds numbers under consideration. The physical correctness of relation (2.4) may be proved by comparing the solutions of the simplified system with the experimental results.

Taking into account that the pressure in equations (2.2) is a function of only x and t we substitute the profile (2.4) into (2.2), and integrating over the y-direction from 0 to $h(x,t)$ gives

$$\frac{\partial q}{\partial t} + 1,2\frac{\partial}{\partial x}\left(\frac{q^2}{h}\right) = gh - \frac{3\nu q}{h^2} + \frac{\sigma h}{\rho}\frac{\partial^3 h}{\partial x^3}, \tag{2.5a}$$

$$\frac{\partial h}{\partial t} + \frac{\partial q}{\partial x} = 0. \tag{2.5b}$$

Here $q = \int_0^h u\,\mathrm{d}y$ and the kinematic condition (2.3) was used in the derivation of (2.5). The system of equations (2.5) was first obtained by Shkadov (1967). In the work presented here the wave regimes of a flowing film will be studied on the basis of (2.5).

The solution of (2.5) related to the Nusselt smooth regime is

$$h = h_N, \quad q = q_N = gh_N^3/3\nu.$$

To investigate its stability with respect to infinitesimal disturbances

$$h = h_N + h', \tag{2.6a}$$

$$q = q_N + q', \tag{2.6b}$$

$$(h', q') \sim \exp\left[\mathrm{i}\alpha(x - ct)\right], \tag{2.6c}$$

the system (2.5) is linearized with respect to h', q' and it is not difficult then to obtain the condition for their resolution:

$$\frac{3(c^* - 3)}{Re_1} + \mathrm{i}\alpha^*(0.2c^{*2} - 1.2(c^* - 1)^2) + \mathrm{i}\alpha^{*3}We_1 = 0. \tag{2.7}$$

Here $c^* = ch_N/q_N$, $\alpha^* = \alpha h_N$, $Re_1 = q_N/\nu$, $We_1 = \sigma h_N/\rho q_N^2$.

Since the stability with respect to disturbances limited throughout the space at any moment of time is here of particular interest, the wavenumber in (2.6) is assumed to be real. Then the values of complex phase velocity c may be found from (2.7). If $\mathrm{Im}(c) > 0$ the disturbance is amplified and if $\mathrm{Im}(c) < 0$ it disappears. As shown by Alekseenko *et al.* (1985) it follows from (2.7) that for any Re_1 there exists a neutral wavenumber α_n^* such that all the disturbances with $\alpha^* < \alpha_n^*$ are unstable and those with $\alpha^* > \alpha_n^*$ disappear. From (2.7) we have

$$\alpha_n^* = \left(\frac{3}{We_1}\right)^{\frac{1}{2}}.$$

The celerity of a neutral disturbance does not depend on wavelength and is equal to

$$c_n^* = 3.$$

Its dimensional wavelength is

$$\lambda_n = \frac{2\pi}{\alpha_n^*} h_N = 2\pi h_N \left(\frac{We_1}{3}\right)^{\frac{1}{2}}.$$

As the small parameter ϵ, introduced above, we may take

$$\epsilon \approx \frac{h_N}{\lambda_n} = \frac{1}{2\pi}\left(\frac{3}{We_1}\right)^{\frac{1}{2}}.$$

It is now possible to estimate the limits of the long-wave approximation. Using the relation for We_1 and Nusselt's formula for q_N it is not difficult to obtain

$$\epsilon \approx \frac{1}{2\pi} 3^{\frac{1}{3}} \left(\frac{Re^5}{Fi}\right)^{\frac{1}{6}}. \tag{2.8}$$

The value of Fi is extremely high for most liquids used in practice. Thus, for water $Fi^{\frac{1}{11}} \approx 10$. It is not difficult to obtain from (2.8) that if $Re \approx 10^2$ then $\epsilon \sim 0.1$.

Using the neutral disturbance wavelength as a scale it is convenient to write the coordinates and variables as follows:

$$h^* = \frac{h}{h_0}, \quad q^* = \frac{q}{q_0}, \quad x^* = \left(\frac{3}{We}\right)^{\frac{1}{2}} \frac{x}{h_0}, \quad t^* = \left(\frac{3}{We}\right)^{\frac{1}{2}} \frac{tq_0}{h_0^2}. \tag{2.9a–d}$$

Then (2.5) become

$$\frac{\partial q^*}{\partial t^*} + 1.2\frac{\partial}{\partial x^*}\left(\frac{q^{*2}}{h^*}\right) = Fh^* - Z\frac{q^*}{h^{*2}} + 3h^*\frac{\partial^3 h^*}{\partial x^{*3}}, \tag{2.10a}$$

$$\frac{\partial h^*}{\partial t^*} + \frac{\partial q^*}{\partial x^*} = 0. \tag{2.10b}$$

Here $Z = (3We/Re^2)^{\frac{1}{2}}$, $F = (We/3Fr^2)^{\frac{1}{2}}$, $We = \sigma h_0/\rho q_0^2$, $Re = q_0/\nu$, $Fr = q_0^2/gh_0^3$.

This variable transformation normalizes the unstable wavenumber range and now $\alpha_n = 1$.

To find nonlinear steady-state travelling solutions of (2.10),

$$h^* = h^*(x^* - c^*t^*), \quad q^* = q^*(x^* - c^*t^*),$$

it is convenient to use the wavelength-averaged thickness and flow rate as scales of h and q, respectively. This choice of scales is more suitable for comparing the calculated and experimental results. As a rule, the Reynolds number based on the mean liquid flow rate is a natural and easily controlled parameter for an experiment on waves travelling down a liquid film and the results are often represented as functions of this parameter. It is evident that the value of F is not predetermined for such a choice of scales, since now the relation between h_0 and q_0 is not prescribed by the Nusselt formula. Therefore, in (2.10) we may fix only one of two parameters, F or Z. The other one may be determined from the solution. Here, the parameter Z will be fixed.

The dimensional variables are determined by the formulae

$$Re = \left(\frac{81Fi}{Z^6}\right)^{\frac{1}{11}}\left(\frac{F}{Z}\right)^{\frac{1}{11}}, \quad c = c^*\left(\frac{\sigma^2 g^3 \nu}{3\rho^2 Z^4}\right)^{\frac{1}{11}}\left(\frac{F}{Z}\right)^{\frac{3}{11}}, \tag{2.11 a, b}$$

$$x = x^*\left(\frac{\sigma^4 \nu^2 Z^3}{g\rho^4 g^5}\right)^{\frac{1}{11}}\left(\frac{F}{Z}\right)^{\frac{5}{11}}, \quad h = h^*\left(\frac{3^5 \sigma \nu^6}{\rho g^4 Z^2}\right)^{\frac{1}{11}}\left(\frac{F}{Z}\right)^{\frac{4}{11}}, \tag{2.11 c, d}$$

$$h_0 = h_{\mathrm{N}}\left(\frac{F}{Z}\right)^{\frac{1}{3}}, \quad h_{\mathrm{N}} = \left(\frac{3\nu^2 Re}{g}\right)^{\frac{1}{3}}. \tag{2.11 e, f}$$

3. Numerical procedure for finding steady-state waves

For steady-state travelling waves equation (2.10*b*) is solved. Taking into account the above-mentioned choice of scales we have

$$q(\xi) = 1 + c(h(\xi) - 1), \quad \xi = x - ct. \tag{3.1}$$

Eliminating the flow rate $q(\xi)$ from equation (2.10*a*) we obtain the equation

$$-c^2\frac{\mathrm{d}h}{\mathrm{d}\xi} + 1.2\frac{\mathrm{d}}{\mathrm{d}\xi}\left[\frac{(1+c(h-1))^2}{h}\right] = Fh - Z\frac{1+c(h-1)}{h^2} + 3h\frac{\mathrm{d}^3 h}{\mathrm{d}\xi^3} \tag{3.2}$$

for $h(\xi)$.

Using the condition $\langle h \rangle = 1$ from (3.2), we find the correlation between F and Z for the periodical solutions:

$$F = Z\left\langle \frac{1+c(h-1)}{h^2} \right\rangle. \tag{3.3}$$

Here the angle brackets denote averaging over a wavelength.

The periodic wave with wavenumber α is presented as a Fourier series

$$h = \sum_{-\infty}^{\infty} h_n \exp[\mathrm{i}\alpha n \xi]. \tag{3.4}$$

Since h is a real function then

$$h_n = \bar{h}_{-n}.$$

The bar denotes the complex conjugate. The relation $h_0 = 1$ is due to the norm condition.

Taking the first $\frac{1}{2}N$ harmonics in the set (3.4), let us substitute this into (3.2) and (3.3). Putting the coefficients with the same exponents equal to zero we obtain a system of $N+1$ complex equations for the real unknowns F, c and N complex ($h_{\pm 1}$, $\ldots, h_{\pm N/2}$):

$$(-c^2 \mathrm{i}\alpha n - F) h_n + 1.2\varphi_n + Z\Psi_n - 3\chi_n = 0, \tag{3.5}$$

$$F = Z\Psi_0,$$

$$n = \pm 1, \pm 2, \ldots \pm \tfrac{1}{2}N.$$

Here φ_n, Ψ_n, χ_n are the Fourier harmonics of

$$\varphi = \frac{\mathrm{d}}{\mathrm{d}\xi}\left[\frac{(1+c(h-1))^2}{h}\right],$$

$$\Psi = \frac{1+c(h-1)}{h^2}, \quad \chi = h\frac{\mathrm{d}^3 h}{\mathrm{d}\xi^3}.$$

Since (3.2) is invariant under a coordinate shift

$$\xi \to \xi + \text{const},$$

the origin of coordinates was chosen such that

$$\mathrm{Im}\,(h_1) = 0.$$

Thus the system (3.5) is complete. The Newton–Kantorovich method was used to solve it numerically. To describe this method briefly, we write the system (3.5) schematically as follows:

$$F_i(x_1^0, x_2^0, \dots x_{N/2}^0), \quad i = 1, \dots \tfrac{1}{2}N. \tag{3.6}$$

Let us take $x^0 = \{x_1^0, \dots, x_{N/2}^0\}$ to be an approximation of the solution of (3.6). Using the Taylor's series representation of the solution of (3.6) in the neighbourhood of x^0 and taking into account only linear terms we obtain equations to find the corrections Δx_i of the x^0 approximation.

These equations are as follows:

$$\left.\frac{\partial F_i}{\partial x_j}\right|_{x=x^0} \Delta x_j = -F_i(x^0).$$

If the x^0 approximation is in the solution attraction region then the numerical procedure converges quickly. The matrix $\partial F_i/\partial x_j$ is computed by use of a difference scheme.

The nonlinear terms φ_n, Ψ_n, χ_n in (3.5) are computed through a pseudo-spectral method, in which a transform to real space is made; the functions φ, Ψ, χ are computed in real space and then a transform back to Fourier space is performed by use of a fast Fourier transformation procedure.

Reducing the set (3.4), the number of harmonics was taken so as to satisfy the relation

$$|h_{N/2}|/\sup |h_n| < 10^{-3}.$$

For this purpose N had to be varied over the range from 16 to 128 depending on the values α and Z.

4. Results of the numerical simulation and comparison with experiments

Periodical steady-state solutions of equation (2.10) with wavenumbers close to the neutral ones were first obtained analytically by Shkadov (1967). Using his results as an initial approximation and taking a small enough step in the parameter α into the region of linear instability, steady-state solutions were found successfully for all values of the parameter Z and the smallest values of α under consideration.

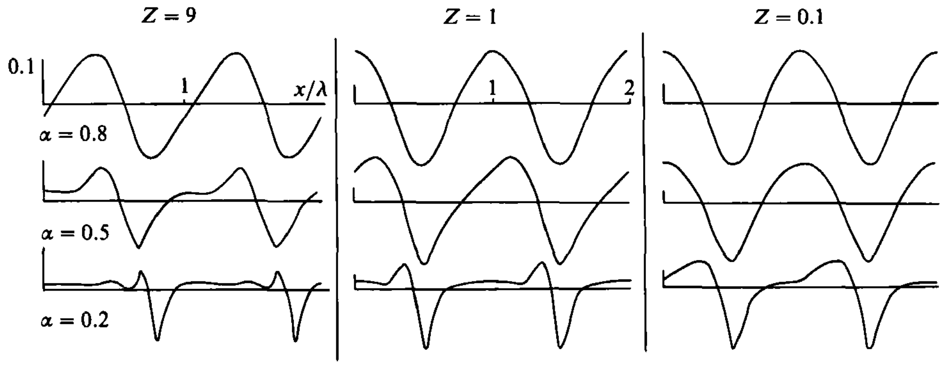

FIGURE 2. Profiles of the wave thickness generated from smooth flow.

Figure 2 shows typical thickness profiles for various values of Z and α. Here the dimensionless thickness is calculated from the mean level and the vertical line corresponds to $h = 0.1$.

As the calculated results show, for every value of α there exists Z^* such that the thickness profile is practically invariant for $Z < Z^*$ (see, for example, figure 2 for $\alpha = 0.8$ and 0.5). For $Z =$ const the thickness profiles are close to a sine wave when the wavenumber is higher than $\alpha^*(Z)$. For $\alpha < \alpha^*$ the difference is more fundamental (see figure 2) and in the limit $\alpha \rightarrow 0$ the waves transform into a series of solitary waves – negative solitons. Shkadov (1977) was the first to find such soliton solutions of (2.10). The waves of this family close to solitary ones have velocities $c < 3$ and there are characteristic oscillations behind the wave.

Chang (1987, 1989) used the normal form method to analyse the bifurcations of Benney's (1966) equation. This approach gives the result that the travelling waves appear from a Hopf bifurcation at the equilibrium point $h = 1$, $h' = 0$, $h'' = 0$ of equations (3.2), as the parameter α decreases through $\alpha = 1$, with Z fixed. The limit cycle expands as α decreases, and disappears at a homoclinic bifurcation as $\alpha \rightarrow 0^+$.

Prior to comparing the calculated and experimental results it is appropriate to describe qualitatively the pattern of waves flowing down a film, using mainly the experiments by Kapitza & Kapitza (1949).

To realize a two-dimensional film flow it is necessary to provide homogeneous conditions of flow over the tube perimeter. The film flow always becomes wavy when the flow rate is above a critical-level, and the wave profile is mainly irregular. Only in rare and accidental circumstances was some periodicity observed when the waves appeared naturally.

If an external periodical impulse was given to the liquid flow not only regular wave profiles but also two basic stable types of wave regimes were observed. The first was termed 'periodical' by Kapitsa (1949). Its thickness profile is close to a sine one for small enough flow rates; the velocity c weakly depends on the liquid flow rate and the wavelength. It was also established that there was some impulse frequency for which the wave pattern was most stable and spread regularly throughout the tube length. This periodical regime appears even for very small external pulses.

The latter types of wave flow regimes develop if the impulses are fewer but larger. In this case one can see how the set of solitary waves begins to run over the tube wall. The shape of a solitary wave consists of 'the base wave' with a sharp front and 'small waves' before the front. The velocity of this type of wave depends essentially on the distance between the solitary waves, as the measurements show.

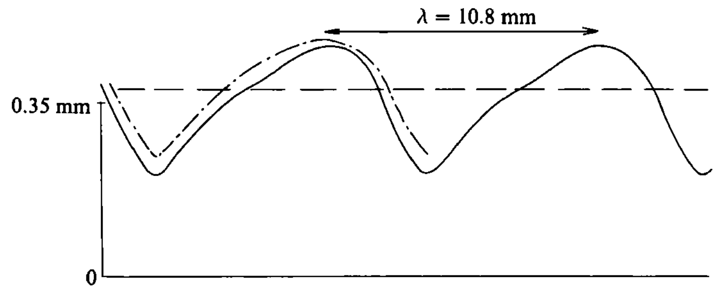

FIGURE 3. Comparison of theoretical (——) and experimental (– – – –) thickness profiles. $Re = 7.2$, $\nu = 4.9 \times 10^{-6}\ \mathrm{m^2/s}$, $\sigma/\rho = 59 \times 10^{-6}\ \mathrm{m^3/s^2}$, $\lambda = 10.8$ mm.

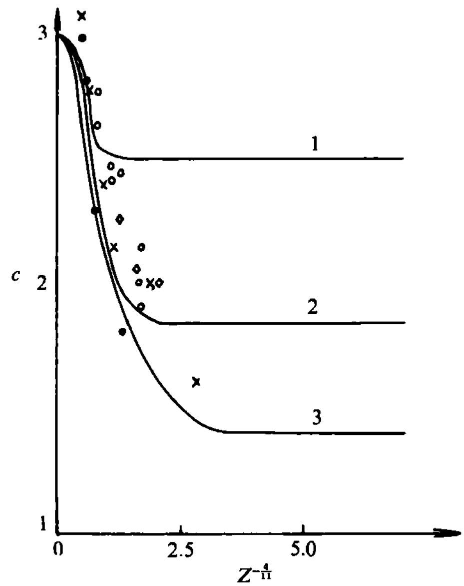

FIGURE 4. Wave velocity *vs.* $Z^{-\frac{4}{11}}$. Theoretical data (curves): line 1, $\alpha = 0.8$; 2, $\alpha = 0.5$; 3, $\alpha = 0.2$. Symbols, experimental data: ●, water ($\nu = 1.14 \times 10^{-6}\ \mathrm{m^2/s}$, $\sigma/\rho = 72.9 \times 10^{-6}\ \mathrm{m^3/s^2}$, $Fi^{\frac{1}{11}} = 8.8$); ○, a water–glycerin film ($\nu = 11.2 \times 10^{-6}\ \mathrm{m^2/s}$, $\sigma/\rho = 55.9 \times 10^{-6}\ \mathrm{m^3/s^2}$, $Fi^{\frac{1}{11}} = 3.56$); ◇, $\nu = 2.16 \times 10^{-6}\ \mathrm{m^2/s}$, $\sigma/\rho = 65.2 \times 10^{-6}\ \mathrm{m^3/s^2}$, $Fi^{\frac{1}{11}} = 6.75$; ×, $\nu = 7.2 \times 10^{-6}\ \mathrm{m^2/s}$, $\sigma/\rho = 57.6 \times 10^{-6}\ \mathrm{m^3/s^2}$, $Fi^{\frac{1}{11}} = 4.21$.

A comparison between the calculated thickness profile (solid line) and the experimental one (dot-dashed line) is illustrated in figure 3. The experimental data were obtained by Nakoryakov *et al.* (1981). Here $Re = 7.2$, $\nu = 4.9 \times 10^{-6}\ \mathrm{m^2/s}$, $\sigma/\rho = 59 \times 10^{-6}\ \mathrm{m^3/s^2}$, $\lambda = 10.8$ mm. The calculated velocity is $c_c = 212$ mm/s, the experimental one is $c_e = 220$ mm/s. These values are in satisfactory agreement.

The calculated long waves of this family have a shape differing from that in the experiment, as illustrated in figure 2.

Calculated wave velocities as functions of Z are presented in figure 4. The greater the value of Z the smaller the value of Re, as follows from (2.11*a*). Here line 1 corresponds to $\alpha = 0.8$, line 2 to $\alpha = 0.5$, and line 3 to $\alpha = 0.2$. The experimental points obtained by Nakorykov *et al.* (1981) corresponding to waves close to sine ones are also presented for water and water-glycerin in this figure. The value of Reynolds number Re varied in this experiment.

The experimental results presented in figure 4 were obtained by imposing

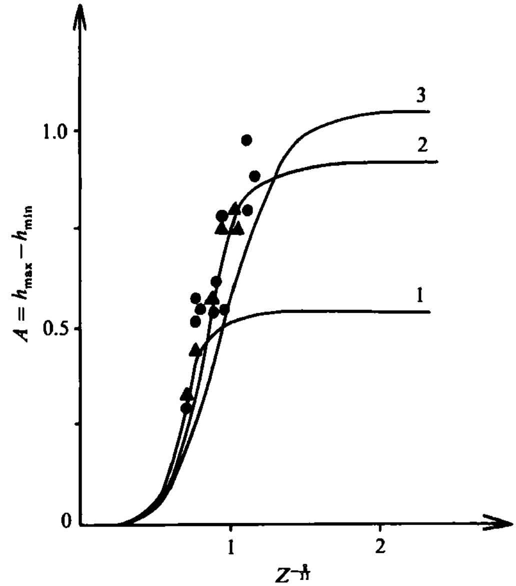

FIGURE 5. Amplitude *vs.* $Z^{-\frac{2}{11}}$. Theoretical data (curves): line 1, $\alpha = 0.8$; 2, $\alpha = 0.5$; 3, $\alpha = 0.2$. Points show experimental data: ●, water, $\nu = 1.14 \times 10^{-6}$ m²/s, $\sigma/\rho = 74 \times 10^{-6}$ m³/s²; ▲, ethyl alcohol, $\nu = 2.02 \times 10^{-6}$ m²/s, $\sigma/\rho = 29 \times 10^{-6}$ m³/s².

pulsations with various frequency and for various liquid flow rates. As follows from figure 4, the wave velocity c depends weakly on α (or on the frequency ω, $\omega = c/\lambda$, $\lambda = 2\pi/\alpha$) in the range of small $Z^{-\frac{4}{11}} \lesssim 1$ (that is small $Re \approx 1.5 Fi^{\frac{1}{11}} Z^{-\frac{6}{11}}$). This agrees with Kapitsa & Kapitsa's experiments. For $Z^{-\frac{4}{11}} \gtrsim 1$ (for water, as an example, this corresponds to $Re \gtrsim 15$) the wavelength dependence becomes more significant. As the flow rate increases, the value of c becomes constant at $Z^{-\frac{4}{11}} \gtrsim Z^{*-\frac{4}{11}}$ if the parameter α is fixed. For waves with $\alpha \gtrsim 0.5$, as seen from figure 4, the following estimate is valid:

$$Z^{*-\frac{4}{11}} \approx 2.$$

For water, it corresponds to $Re \approx 30$.

The analogous dependence of the wave amplitude $A = h_{max} - h_{min}$ on Z for the same values of wavenumber α as in figure 4, are presented in figure 5. Here the points correspond to the experimental results of Kapitza for water and ethyl alcohol. There is a good agreement between the theory and experiment here too. The amplitude of steady-state waves sharply increases, beginning from a non-zero value of $Z^{-\frac{2}{11}}$, as is demonstrated by figure 5. This fact explains to some extent the critical Reynolds number, Re_*, of wave formation in the experiments. To compare the critical Re_* determined theoretically and experimentally it is convenient to use the formula suggested by Kapitza:

$$Re_* = 0.61 Fi^{\frac{1}{11}}.$$

Using (2.11) and taking into account the approximation $F \approx Z$, this formula may be written as

$$Z_*^{-\frac{2}{11}} \approx 0.74.$$

This value of Z corresponds to $A \approx 0.2$ in figure 5. It is interesting to note that Z_* corresponds closely to the beginning of a sharp variation in the variable $(F/Z)^{\frac{1}{3}}$ (figure 6). Here lines 1–3 correspond to the same values of α as in figures 4 and 5.

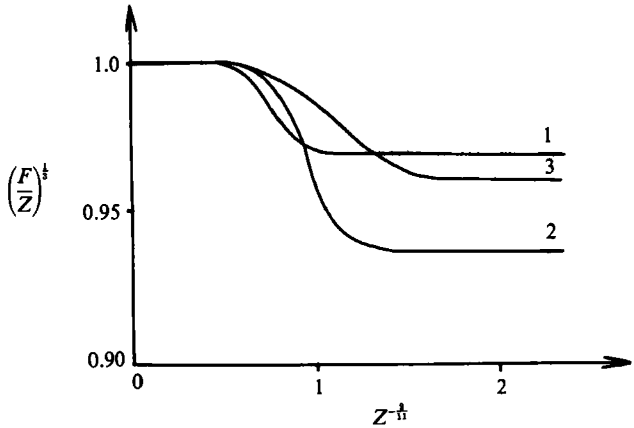

FIGURE 6. Relation between the dimensional and Nusselt mean thicknesses *vs.* $Z^{-\frac{2}{11}}$. Theoretical data: line 1, $\alpha = 0.8$, 2, $\alpha = 0.5$; 3, $\alpha = 0.2$.

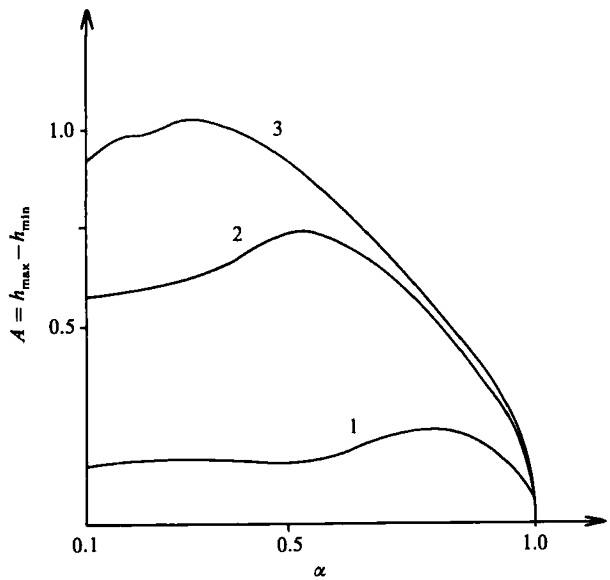

FIGURE 7. Amplitude *vs.* α. Theoretical data: line 1, $Z = 10$; 2, $Z = 1$; 3, $Z = 0.1$.

The amplitudes as functions of the wavenumber α for three characteristic values of Z are presented in figure 7. Here line 1 corresponds to $Z = 10$, 2 corresponds to $Z = 1$, and 3 corresponds to $Z = 0.1$. As follows from figure 7, the branching of new regimes from the solution $h = 1$ is of a soft type and the dependence $A(\alpha)$ has a maximum. The amplitude $A(\alpha)$ becomes constant if α decreases and the solution, as it was mentioned above, transforms into a set of solitary waves if $\alpha \rightarrow 0$.

The dependences of c and $(F/Z)^{\frac{1}{3}}$ on α for the same values of Z as in figure 7 are presented in figures 8 and 9 respectively. The velocity of the waves is always less than 3 $c < 3$, as is shown in figure 8.

The results presented above describe quite fully the steady-state travelling wave solutions of (2.10), branching from the smooth flow. The waves close to sine ones which were observed in the experiments correspond well quantitatively to some waves of this one-parameter family.

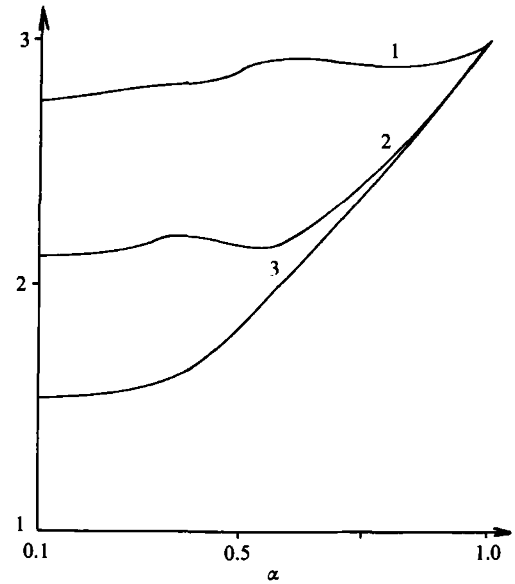

FIGURE 8. Wave velocity *vs.* α. Theoretical data: line 1, $Z = 10$; 2, $Z = 1$; 3, $Z = 0.1$.

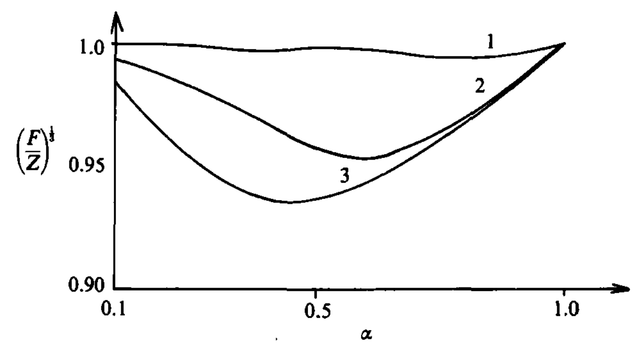

FIGURE 9. Relation between the dimensional and Nusselt mean thicknesses *vs.* α. Theoretical data: line 1, $Z = 10$; 2, $Z = 1$; 3, $Z = 0.1$.

To determine which waves of this family can be experimentally seen it is necessary, as a minimum, to study the stability of the waves.

5. The method of studying the stability of nonlinear wave regimes

Substituting $h = h_0(\xi)+h'(\xi,t)$, $q = q_0(\xi)+q'(\xi,t)$ into (2.10) and linearizing it we obtain the system

$$\frac{\partial q}{\partial t}-c\frac{\partial q}{\partial \xi}-1.2\frac{q_0^2}{h_0^2}\frac{\partial h}{\partial \xi}+2.4\frac{q_0}{h_0}\frac{\partial q}{\partial \xi}+\left(2.4\frac{\mathrm{d}}{\mathrm{d}\xi}\frac{q_0}{h_0}+\frac{Z}{h_0^2}\right)q$$

$$-3h_0\frac{\partial^3 h}{\partial \xi^3}-\left(1.2\frac{\mathrm{d}}{\mathrm{d}\xi}\frac{q_0^2}{h_0^2}+F+2Z\frac{q_0}{h_0^3}+3\frac{\mathrm{d}^3 h_0}{\mathrm{d}\xi^3}\right)h = 0, \quad (5.1a)$$

$$\frac{\partial h}{\partial t}-c\frac{\partial h}{\partial \xi}+\frac{\partial q}{\partial \xi} = 0, \quad (5.1b)$$

to study the stability of the steady-state solution $h_0(\xi)$, $q_0(\xi)$. Here the primes on disturbance values are omitted.

Since the variable t is not explicitly incorporated in (5.1) the solution may be represented as

$$h = \mathrm{e}^{-\gamma t} h_1(\xi), \quad q = \mathrm{e}^{-\gamma t} q_1(\xi). \tag{5.2a, b}$$

Then the system of ordinary linear differential equations with periodic coefficients for h_1, q_1 is

$$-\gamma q_1 - c\frac{\mathrm{d}q_1}{\mathrm{d}\xi} - 1.2\frac{q_0^2}{h_0^2}\frac{\mathrm{d}h_1}{\mathrm{d}\xi_1} + 2.4\frac{q_0}{h_0}\frac{\mathrm{d}q_1}{\mathrm{d}\xi} + \left(2.4\frac{\mathrm{d}}{\mathrm{d}\xi}\frac{q_0}{h_0} + \frac{Z}{h_0^2}\right)q_1$$

$$-3h_0\frac{\mathrm{d}^3h_1}{\mathrm{d}\xi^3} - \left(1.2\frac{\mathrm{d}}{\mathrm{d}\xi}\frac{q_0^2}{h_0^2} + F + 2Z\frac{q_0}{h_0^3} + 3\frac{\mathrm{d}^3h_0}{\mathrm{d}\xi^3}\right)h_1 = 0, \tag{5.3a}$$

$$-\gamma h_1 - c\frac{\mathrm{d}h_1}{\mathrm{d}\xi} + \frac{\mathrm{d}q_1}{\mathrm{d}\xi} = 0. \tag{5.3b}$$

Since the disturbances are initially limited for all values of ξ, solutions of (5.3) which are also limited for all ξ are of particular interest here. It follows from Floquet's theorem that such solutions are of the form

$$h_1 = \varphi(\xi)\,\mathrm{e}^{\mathrm{i}\alpha Q\xi}, \quad q_1 = \Psi(\xi)\,\mathrm{e}^{\mathrm{i}\alpha Q\xi}, \tag{5.4a, b}$$

where φ, Ψ are the periodical functions of the same period as $h_0(\xi)$, $q_0(\xi)$, and Q is a real parameter. Substituting (5.4) into (5.3) we obtain

$$-\gamma\Psi + (A + \mathrm{i}\alpha QB)\,\Psi + B\frac{\mathrm{d}\Psi}{\mathrm{d}\xi} - (P + \mathrm{i}\alpha QD - 3\mathrm{i}\alpha^3Q^3h_0)\,\varphi$$

$$-(D - 9\alpha^2Q^2h_0)\frac{\mathrm{d}\varphi}{\mathrm{d}\xi} - 9\mathrm{i}\alpha Qh_0\frac{\mathrm{d}^2\varphi}{\mathrm{d}\xi^2} - 3h_0\frac{\mathrm{d}^3\varphi}{\mathrm{d}\xi^3} = 0, \tag{5.5a}$$

$$-\gamma\varphi + \mathrm{i}\alpha Q\Psi + \frac{\mathrm{d}\Psi}{\mathrm{d}\xi} - \mathrm{i}\alpha Qc\varphi - c\frac{\mathrm{d}\varphi}{\mathrm{d}\xi} = 0, \tag{5.5b}$$

where
$$A = 2.4\frac{\mathrm{d}}{\mathrm{d}\xi}\left(\frac{q_0}{h_0}\right) + \frac{Z}{h_0^2}, \quad B = 2.4\frac{q_0}{h_0} - c$$

$$P = 1{,}2\frac{\mathrm{d}}{\mathrm{d}\xi}\left(\frac{q_0^2}{h_0^2}\right) + F + 2Z\frac{q_0}{h_0^3} + 3\frac{\mathrm{d}^3h_0}{\mathrm{d}\xi^3}, \quad D = 1.2\frac{q_0^2}{h_0^2}.$$

Thus the investigation of the stability of periodic steady-state travelling wave solutions $h_0(\xi)$, $q_0(\xi)$ with respect to infinitesimal two-dimensional disturbances is reduced to studying the spectrum of those eigenvalues for different values Q for which (5.5) has periodic solutions of the same period as for h_0, q_0. The wave is stable if, for any Q, all γ have $\mathrm{Re}\,(\gamma) \geqslant 0$.

It follows from (5.4) that it is sufficient to consider Q within any interval of unit length, for example $[-0.5; 0.5]$. Taking the complex conjugate of (5.5) it is easy to become convinced that $\gamma(Q) = \bar{\gamma}(-Q)$. Thus it is sufficient to consider the solutions (5.5) for $0 \leqslant Q \leqslant 0.5$.

The results which were obtained for $Q = 0$ describe the stability with respect to special but important class of disturbances. They have the same period as the wave flow under consideration. In this case one of the solutions of (5.5) is readily found analytically:

$$\gamma = 0, \quad \varphi = h_0', \quad \Psi = q_0'. \tag{5.6}$$

This result is a consequence of Andronov–Vitt's theorem concerning the presence of at least one zero Lyapunov's index for a closed trajectory. To find the other γ the problem was solved numerically in the general case $Q \neq 0$.

After Fourier transforming (5.5), we obtain an infinite system of linear algebraic homogeneous equations to determine φ_n, Ψ_n. Setting all $\varphi_n, \Psi_n (|n| > \frac{1}{2}N)$ equal to zero, we obtain its finite approximation:

$$\sum_{k=-\frac{1}{2}N}^{\frac{1}{2}N} (V_{n-k}\Psi_k + W_{n-k}\varphi_k) = \gamma \Psi_n, \tag{5.7}$$

$$(\mathrm{i}\alpha Q + \mathrm{i}\alpha n)\Psi_n - (\mathrm{i}\alpha Q c + \mathrm{i}\alpha c n)\varphi_n = \gamma\varphi_n,$$

$$n = -\tfrac{1}{2}N/2, \ldots, \tfrac{1}{2}N.$$

Here
$$V_{n-k} = (A + \mathrm{i}\alpha Q B)_{n-k} + \mathrm{i}\alpha k B_{n-k},$$

$$W_{n-k} = -(P + \mathrm{i}\alpha Q D - 3\mathrm{i}\alpha^3 Q^3 h_0)_{n-k} - \mathrm{i}\alpha k (D - 9\alpha^2 Q^2 h_0)_{n-k} + (9\mathrm{i}\alpha^3 Q k^2 + 3\mathrm{i}\alpha^3 k^3)\, h_{0_{n-k}}.$$

6. An analytical investigation of long-disturbance stability

As calculations show, the long modulated disturbances with $Q \ll 1$ are important in that they are responsible for the sizes of stability zones, if any. Analytical methods may be used to investigate the increments of such disturbances. In order to emphasize that only small Q are considered in this section this parameter will be denoted by ϵ.

Introducing the set of fast and slow variables

$$\xi_0 = \xi, \quad \xi_1 = \epsilon\xi,$$
$$t_n = \epsilon^n t, \quad n = 1, 2,$$

one expands the solution of (2.10) as

$$q = q_0 + \epsilon q_1 + \epsilon^2 q_2 + \epsilon^3 q_3 + \ldots,$$
$$h = h_0 + \epsilon h_1 + \epsilon^2 h_2 + \epsilon^3 h_3 + \ldots.$$

Here $q_0(\xi)$, $h_0(\xi)$, the wave velocity c and the value of F have been previously determined. Functions $q_1, q_2, q_3, \ldots, h_1, h_2, h_3 \ldots$ depend on fast and slow variables. Further, we shall consider only those solutions for which the functions $q_n, h_n (n = 1, 2 \ldots)$ depend on the fast variable ξ_0 periodically with period $2\pi/\alpha$, where α is the wavenumber of the q_0, h_0 solution.

In the first power of ϵ we have

$$-c\frac{\partial q_1}{\partial \xi_0} + 1.2\frac{\partial}{\partial \xi_0}\left(\frac{q_0^2}{h_0}\left(2\frac{q_1}{q_0} - \frac{h_1}{h_0}\right)\right) - F h_1 + Z\frac{q_0}{h_0^2}\left(\frac{q_1}{q_0} - 2\frac{h_1}{h_0}\right) - 3h_0\frac{\partial^3 h_1}{\partial \xi_0^3} - 3h_1\frac{\mathrm{d}^3 h_0}{\mathrm{d}\xi_0^3} = 0 \tag{6.1a}$$

$$-c\frac{\partial h_1}{\partial \xi_0} + \frac{\partial q_1}{\partial \xi_0} = 0. \tag{6.1b}$$

Its non-trivial solution is (5.6):

$$q_1 = A\frac{\mathrm{d}q_0}{\mathrm{d}\xi}, \quad h_1 = A\frac{\mathrm{d}h_0}{\mathrm{d}\xi};$$

here A is a function of the slow variables.

In the second approximation, we have the inhomogeneous system

$$\mathrm{L}\begin{pmatrix} q_2 \\ h_2 \end{pmatrix} = \begin{pmatrix} f_1 \\ f_2 \end{pmatrix}, \tag{6.2}$$

$$f_1 = -\frac{\partial q_1}{\partial t_1} + c\frac{\partial q_1}{\partial \xi_1} - 1.2\frac{\partial}{\partial \xi_0}\left[\frac{q_0^2}{h_0}\left(\frac{q_1}{q_0} - \frac{h_1}{h_0}\right)^2\right] - 1.2\frac{\partial}{\partial \xi_1}\left[\frac{q_0^2}{h_0^2}\left(2\frac{q_1}{q_0} - \frac{h_1}{h_0}\right)\right]$$
$$- Z\frac{q_0}{h_0^2}\left(\frac{3h_1^2}{h_0^2} - \frac{2h_1 q_1}{h_0 q_0}\right) + 3\left(3h_0\frac{\partial^3 h_1}{\partial \xi_0^2 \partial \xi_1} + h_1\frac{\partial^3 h_1}{\partial \xi_0^3}\right);$$

$$f_2 = -\frac{\partial h_1}{\partial t_1} + c\frac{\partial h_1}{\partial \xi_1} - \frac{\partial q_1}{\partial \xi_1}.$$

Here L is the linear differential operator of (6.1).

To solve (6.2), it follows from general theory that the right-hand side of (6.2) should be orthogonal to the solutions of a homogeneous problem conjugated with (6.1). Multiplying (6.1*a*) by Ψ and (6.1*b*) by φ, summing them and integrating over ξ_0 from 0 to λ, the equations of the conjugated problem are readily obtained:

$$c\frac{\partial \psi}{\partial \xi_0} - \frac{\partial \varphi}{\partial \xi_0} - 2.4\frac{q_0}{h_0}\frac{\partial \Psi}{\partial \xi_0} + Z\frac{\Psi}{h_0^2} = 0,$$

$$1.2\frac{q_0^2}{h_0^2}\frac{\partial \Psi}{\partial \xi_0} + c\frac{\partial \varphi}{\partial \xi_0} - F\Psi - 2Z\frac{q_0}{h_0^3}\Psi - 3\Psi\frac{\partial^3 h_0}{\partial \xi_0^3} + 3\frac{\partial^3}{\partial \xi_0^3}(h_0\Psi) = 0.$$

One of its solutions may be written as

$$(\Psi^*, \varphi^*) = (0, 1). \tag{6.3}$$

It was verified by a numerical investigation of the spectrum of the conjugated operator L that there are no other non-trivial solutions of the conjugated problem at non-specific points.

The right-hand part of (6.2) is clearly orthogonal to (6.3). As system (6.2) is linear, its solutions may be presented as

$$q_2 = \alpha_1\frac{\partial A}{\partial t_1} + \beta_1\frac{\partial A}{\partial \xi_1} + \gamma_1 A^2, \tag{6.4a}$$

$$h_2 = \alpha_2\frac{\partial A}{\partial t_1} + \beta_2\frac{\partial A}{\partial \xi_1} + \gamma_2 A^2. \tag{6.4b}$$

The functions $\alpha_1, \beta_1, \gamma_1, \alpha_2, \beta_2, \gamma_2$ depend on the variable ξ_0 and may be found numerically. The equations for these functions are obtained by substituting (6.4) in (6.2), giving three systems of inhomogeneous ordinary differential equations for the functions (α_1, α_2), (β_1, β_2), (γ_1, γ_2) to calculate. The left-hand side of these systems is that of (6.1) with (q_1, h_1) replaced by (α_1, α_2), (β_1, β_2), (γ_1, γ_2), respectively. Since the solution of the homogeneous system may be added to that of the inhomogeneous one, the normalizing conditions of orthogonality were used:

$$\int_0^\lambda \left(\alpha_1 \frac{dq_0}{d\xi} + \alpha_2 \frac{dh_0}{d\xi}\right) d\xi = 0,$$

$$\int_0^\lambda \left(\beta_1 \frac{dq_0}{d\xi} + \beta_2 \frac{dh_0}{d\xi}\right) d\xi = 0,$$

$$\int_0^\lambda \left(\gamma_1 \frac{dq_0}{d\xi} + \gamma_2 \frac{dh_0}{d\xi}\right) d\xi = 0.$$

By use of the Fourier transformation the differential equations reduced to linear algebraic ones.

The following inhomogeneous system of equations is obtained for the third approximation:

$$\mathrm{L}(q_3, h_3) = (g_1, g_2) \tag{6.5}$$

$$\begin{aligned} g_1 = & -\frac{\partial q_1}{\partial t_2} - \frac{\partial q_2}{\partial t_1} + c\frac{\partial q_1}{\partial \xi_2} + c\frac{\partial q_2}{\partial \xi_1} - \chi \frac{\partial}{\partial \xi_0} \\ & \times \left[\frac{q_0^2}{h_0}\left(2\left(\frac{q_1 q_2}{q_0^2} + \frac{h_1 h_2}{h_0^2} - \frac{q_2 h_1}{q_0 h_0} - \frac{q_1 h_2}{q_0 h_0}\right) - \frac{h_1}{h_0}\left(\frac{q_1}{q_0} - \frac{h_1}{h_0}\right)^2\right)\right] \\ & -\chi \frac{\partial}{\partial \xi_1}\left[\frac{q_0^2}{h_0}\left(\frac{2q_2}{q_0} - \frac{h_2}{h_0} + \left(\frac{q_1}{q_0} - \frac{h_1}{h_0}\right)^2\right)\right] - \chi\frac{\partial}{\partial \xi_2}\left[\frac{q_0^2}{h_0}\left(\frac{2q_1}{q_0} - \frac{h_1}{h_0}\right)\right] \\ & -Z\frac{q_0}{h_0^2}\left(-4\frac{h_1^3}{h_0^3} + \frac{3q_1 h_1^2}{q_0 h_0^2} + \frac{6h_1 h_2}{h_0^2} - \frac{2h_2 h_1}{h_0 q_0} - \frac{2q_2 h_1}{q_0\, h_0}\right) \\ & +3\left(h_2 \frac{\partial^3 h_1}{\partial \xi_0^3} + h_1 \frac{\partial^3 h_2}{\partial \xi_0^3} + 3h_1 \frac{\partial^3 h_1}{\partial \xi_0^2 \partial \xi_1} + 3h_0\left(\frac{\partial^3 h_2}{\partial \xi_0^2 \partial \xi_1} + \frac{\partial^3 h_1}{\partial \xi_1^2 \partial \xi_0} + \frac{\partial^3 h_1}{\partial \xi_0^2 \partial \xi_2}\right)\right); \end{aligned}$$

$$g_2 = -\frac{\partial h_1}{\partial t_2} - \frac{\partial h_2}{\partial t_1} + c\frac{\partial h_1}{\partial \xi_2} + c\frac{\partial h_2}{\partial \xi_1} - \frac{\partial q_1}{\partial \xi_2} - \frac{\partial q_2}{\partial \xi_1}.$$

The orthogonality condition of the right-hand side of equation (6.5) to the solution of (6.3) is $\langle g_2 \rangle = 0$, where $\langle\ \rangle$ denotes the wavelength average.

The linear part of the resulting equation with respect to the function $A(t_1, \xi_1)$ is in the form

$$-\langle\alpha_2\rangle \frac{\partial^2 A}{\partial t_1^2} - (\langle\beta_2\rangle - c\langle\alpha_2\rangle + \langle\alpha_1\rangle)\frac{\partial^2 A}{\partial t_1 \partial \xi_1} - (\langle\beta_1\rangle - c\langle\beta_2\rangle)\frac{\partial^2 A}{\partial \xi_1^2} = O(A). \tag{6.6}$$

To investigate the stability of q_0, h_0 the nonlinear term $O(A)$ is neglected. Substituting into (6.6)

$$A \sim e^{-\eta t_1} e^{i\xi_1},$$

we obtain a quadratic equation for the complex value η, from where it follows for $a = \mathrm{Re}(\eta)$ that

$$a^2 = -R_x = \frac{\langle\beta_1\rangle - c\langle\beta_2\rangle}{\langle\alpha_2\rangle} - \frac{(\langle\beta_2\rangle - c\langle\alpha_2\rangle + \langle\alpha_1\rangle)^2}{4\langle\alpha_2\rangle^2}. \tag{6.7}$$

If $R_x < 0$, it is obvious that A increases with time, and the solution q_0, h_0 is unstable. If $R_x > 0$, η takes an imaginary value. In this case, it is necessary to consider one more approximation. Omitting intermediate considerations, let us analyse the linear part of the equation following from the orthogonality condition:

$$-2\langle\alpha_2\rangle\frac{\partial^2 A}{\partial t_2\,\partial t_1}-(\langle\beta_1\rangle-c\langle\alpha_2\rangle+\langle\alpha_1\rangle)\frac{\partial^2 A}{\partial t_2\,\partial\xi_1}-\langle b\rangle\frac{\partial^3 A}{\partial t_1^3}-(\langle\mu_1\rangle-c\langle\mu\rangle)\frac{\partial^3 A}{\partial\xi_1^3}$$
$$-(\langle d\rangle-c\langle b\rangle+\langle b_1\rangle)\frac{\partial^3 A}{\partial t_1^2\,\partial\xi_1}-(\langle\mu\rangle-c\langle d\rangle+\langle d_1\rangle)\frac{\partial^3 A}{\partial t_1\,\partial\xi_1^2}=0. \quad (6.8)$$

Here μ, μ_1, b, b_1, d, d_1 are functions of ξ_0, obtained from the solution of the system when ϵ^3.

Substituting into (6.8)

$$A \sim \exp[-\eta_1 t_2-\eta t_1+\mathrm{i}\xi_1], \quad (6.9)$$

to determine η_1 we arrive at a linear equation. It should be noted that since the quadratic equation to determine η is obtained from (6.7), both solutions of this equation have to be substituted one after the other into (6.8) instead of η, and then the two values η_1^1 and η_1^2 have to be found. If Re (η_1^1) and Re (η_1^2) are greater than zero, the initial solution is stable, and if at least one of these real parts is less than zero, it is unstable.

7. Results on nonlinear-regime stability

The calculations on nonlinear-regime stability have shown that disturbances of the same periodicity are less dangerous than in the linear regime. Thus, for $Q = 0$ a range of steady wavenumbers exists for every Z. It is quite wide – from the upper boundary of linear instability of a plane-parallel flow, $\alpha = 1$, to the values of wavenumbers shown by Curve 1 on figure 10.

The solutions under investigation are stable with respect to disturbances with $Q \neq 0$ over a narrower range of wavenumbers and only for sufficiently high values of Z and respectively low Re. The stability zone is shown in figure 10 by hatching.

For nonlinear regimes with the wavenumbers lying on Curve 1 (figure 10) a neutral disturbance with $Q = 0$ exists for which Im $(\gamma) \neq 0$. This type of stability change corresponds to a Landau–Hopf bifurcation. The value of instability increment quickly increases below Curve 1, which is responsible, among other factors, for the absence of long waves such as 'succession of negative solitons'.

The region of wave regimes stable with respect to disturbances with various Q for $Z = 5$ is shown shaded in figure 11 (a). Here the behaviour of the real parts of the first four eigenvalues for different values of α is also shown (figure 11b). As is seen, the stability is defined by the behaviour of two eigenvalues which start from zero when $Q = 0$. This passage through zero determines the respective upper and lower boundaries of the stability region. Neutral disturbances on the boundaries of this region are of different type. On the upper boundary an imaginary part of the eigenvalue is equal to zero and on the lower one the neutral disturbance has an oscillating component in time.

As is seen from figure 12, as Z decreases, the interval of steady waves becomes narrower and shifts to smaller α.

When $Z < Z_{**} = 4$ the stability region deviates from the axis $Q = 0$, i.e. for such Z there are always Q for which increasing disturbances are available at every α value.

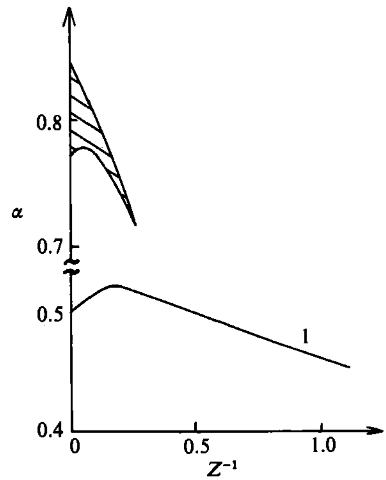

FIGURE 10. The hatched region shows the zone of wave regimes stable with respect to two-dimensional disturbances. Between line $\alpha = 1$ and line 1 the waves are stable with respect to disturbances of the same period.

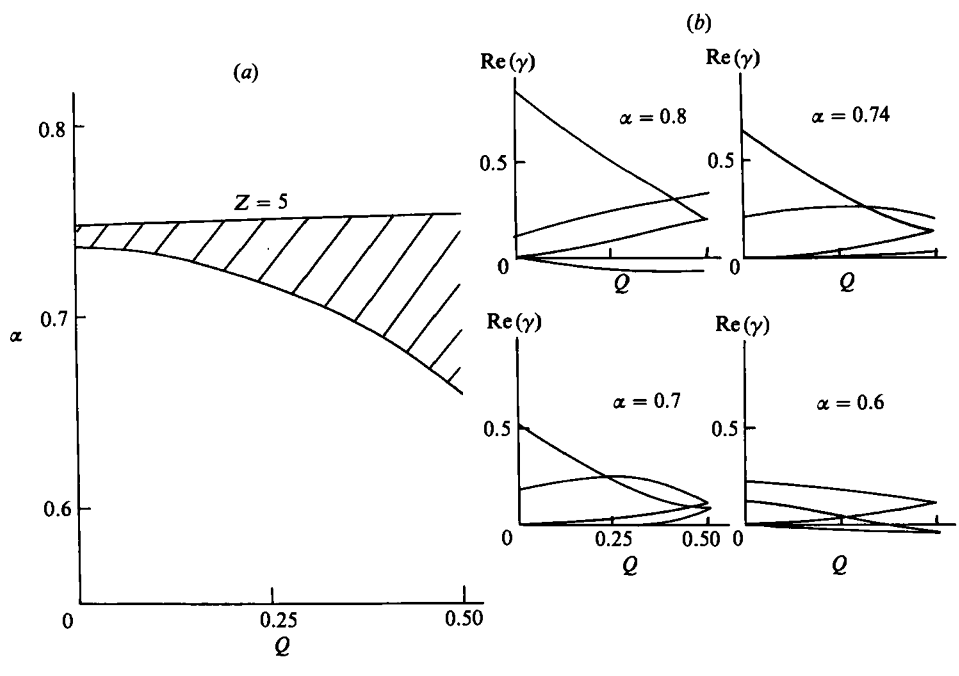

FIGURE 11. (*a*) The hatched region shows the zone of wave regimes stable with respect to disturbances with various Q. (*b*) The behaviour of increments of the four most dangerous disturbances *vs*. Q.

The calculated results are compared with the experimental data in figure 5. A value of $Z_{**}^{-\frac{2}{11}} = 0.78$ is somewhat higher than the critical number for wave formation, $Z_*^{-\frac{2}{11}} \approx 0.74$; however, as follows from the experiments, sinusoidal waves similar to steadily travelling ones are also observed when $Z < Z_*$ (figure 5). Thus, the instability to disturbances with $Q \neq 0$ does not mean that such waves are impossible

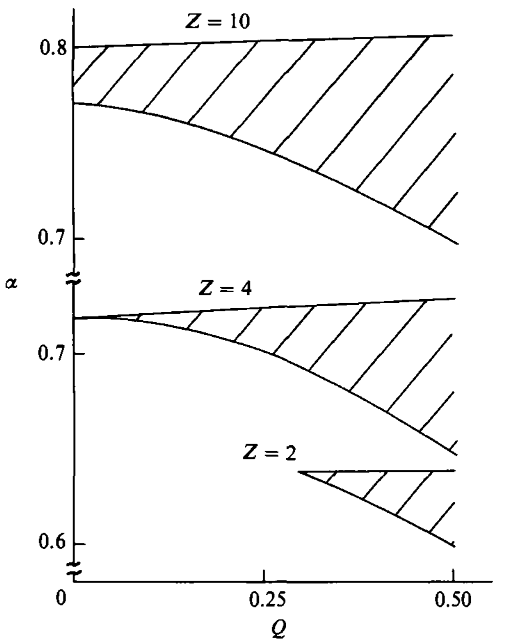

FIGURE 12. The hatched regions show zones of wave regimes stable with respect to disturbances with various Q.

to observe experimentally. However, the regimes unstable with respect to disturbances with $Q = 0$ are not realized experimentally.

As follows from the results of calculations, sinusoidal waves are practically always unstable. Nevertheless, the data obtained by Alekseenko *et al.* (1985) show that there is a particular difference between the regimes' stability. To interpret these data it is appropriate to analyse the values of increments for increasing disturbances.

The cross-hatching in figure 13 shows the region of stable wavenumbers and the single hatching shows the region where disturbances grow rather slowly, and in this case the growth rate is $\delta = -\text{Re}(\gamma) < 10^{-2}$. For the water–glycerine mixture, for example, they slightly distort a wave flow up to the distance $l \approx 10$–20 cm. Such regimes may be classified from an experimental point of view as steady-state travelling waves. Some experimental data can be explained more clearly if one postulates the assumption, which seems reasonable, that the external pulsations, cause a wave regime with a definite α do not allow disturbances with Q strongly differing from zero and, on the other hand, disturbances with small Q occur owing to the instability of the external pulsation generator. Thus, it becomes clear why an excited wave exists over greater distances than a naturally generated one. Disturbances with Q strongly differing from zero, which can occur for natural waves, make the waves unstable more quickly (their increment is much higher than that of the disturbances with small Q (see figure 11)). For the same reason, excited waves are observed over a wider range of wavenumbers. Also, since the upper boundary of weakly growing disturbances is close to the stability boundary for most Q, except for very low values $Q < Q_*$ (it may assumed that the generation of excited waves results in small $Q > Q_*$), it is evident that expansion must be towards lower wavenumbers (figure 13). This was observed experimentally Alekseenko *et al.* (1985).

Figure 14 displays the values of R_x, $\text{Re}(\eta_1^1)$ and $\text{Re}(\eta_1^2)$ for the first family for $Z =$

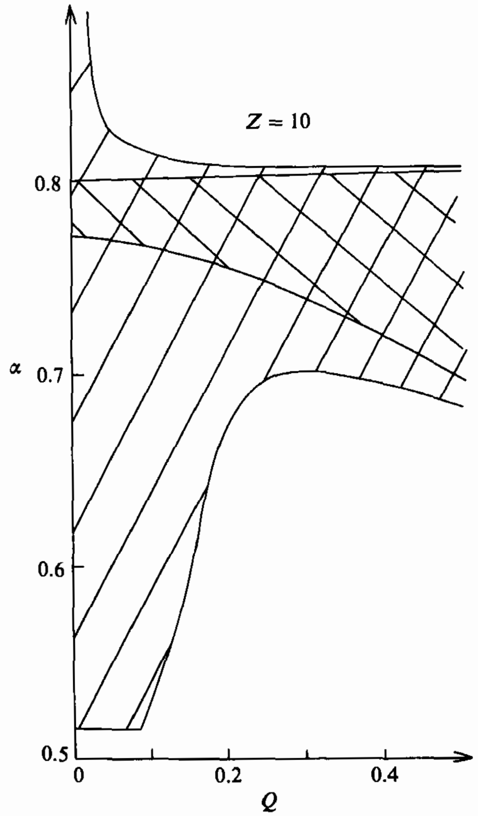

FIGURE 13. The hatched region shows the zone of wave regimes where the unstable disturbances grow slowly ($\delta = -\mathrm{Re}\,(\gamma) < 10^{-2}$). The cross-hatching shows zones of wave regimes stable with respect to disturbances with various Q.

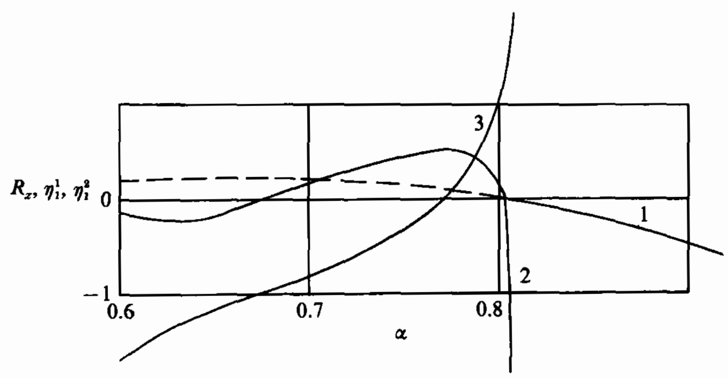

FIGURE 14. Results concerning the stability of wave regimes with respect to long modulated disturbances (small Q). Here $Z = 10$. If $R_x < 0$ (line 1) then the disturbances are increasing and the value of increment $\sim Q$. If $R_x > 0$ then the stability is determined by values of $\mathrm{Re}\,(\eta_1^1)$ and $\mathrm{Re}\,(\eta_1^2)$ (lines 2 and 3), the value of the disturbance increment $\sim Q^2$.

10 versus the wavenumber (R_x is plotted by line 1, $\mathrm{Re}\,(\eta_1^1)$ by line 2 and $\mathrm{Re}\,(\eta_1^2)$ by line 3). For $R_x > 0$ line 1 is dashed, since at those points the stability is defined by $\mathrm{Re}\,(\eta_1^1)$ and $\mathrm{Re}\,(\eta_1^2)$. The results presented in figure 14 are in agreement with those presented in figure 13.

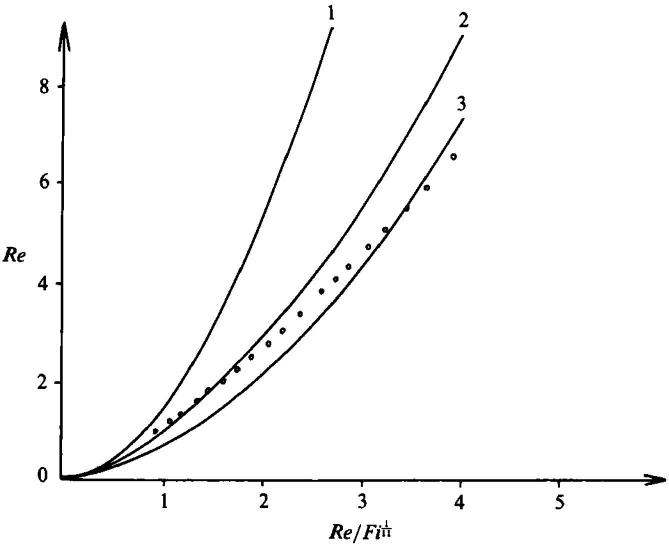

FIGURE 15. Line 1, the neutral curve for smooth flow. Line 2, the neutral curve for the most dangerous disturbances with small Q, that is $R_x = 0$. Line 3, Landau–Hopf bifurcation. This line corresponds to line 1 in figure 10. Points show the upper bound of existence of excited waves from experiments.

As follows from (6.9) and figure 14, when the disturbance increments are beyond the range of stable wavenumbers α on the lower boundary (where line 3 intersects the abscissa axis) they grow more slowly ($\sim\epsilon$) than on the upper boundary which almost coincides with the root of curve 1, where the increments grow $\sim\epsilon^2$. Thus, as was mentioned in §6, the unstable disturbances above the upper boundary of the stability zone and, respectively, under the lower one are of different types. The disturbances having the increment of $\sim\epsilon$ are more dangerous.

Figure 15 illustrates the comparison between the calculated data on the first-family wave stability and the upper bound of existence of excited waves found by Alekseenko *et al.* (1985). The experimental data are shown here by dots; line 1 is a neutral stability curve of plane-parallel flow down a slope, line 2 is a neutral curve for the most dangerous disturbances with small Q, i.e. $R_x = 0$, line 3 corresponds to line 1 in figure 10 and it is the line of wave stability with respect to disturbances of the same period as that of basic wave. As is shown in figure 15, lines 2 and 3 correspond rather well to the experimental boundary of the existence of excited waves.

8. Some remarks

The investigation of the stability of stationary waves bifurcating from a plane-parallel regime allows the following conclusions to be drawn:

(i) The solutions with wavenumbers lying between lines 1 and 3 (figure 15) may be distinguished in a narrow sense of stability. They are stable with respect to disturbances of the same periodicity.

(ii) Regimes that are stable with respect to all plane disturbances, exist only for low Re ($Z > 4$).

(iii) The length-modulated disturbances (small Q) are of great significance from the viewpoint of experimental realization. Perturbation theory shows that there exist two types of disturbances whose instability growth rates differ by an order of magnitude. The wave regimes between lines 1 and 2 (figure 15) are more unstable.

The results obtained explain some experimental phenomena such as the difference in the evolution of naturally generated and excited waves and why long waves like a succession of negative solitons are not observed experimentally. Also, it becomes more clear why the external pulsations increase the region of steady-state travelling waves and expand possible wave regimes towards lower wavenumbers.

The calculations on stability made it possible to narrow the range of possible wave regimes.

The obtained results on stability allow a detailed bifurcation analysis of waves belonging to this family to be made and new types of periodic waves to be found.

REFERENCES

ALEKSEENKO, S. V., NAKORYAKOV, V. YE. & POKUSAEV, B. G. 1985 Wave formation on a vertical falling liquid film. *AIChE J.* **31**, 1446–1460.

BACH, P. & VILLADSEN, J. 1984 Simulation of the vertical flow of a thin wavy film using a finite-elements method. *Intl J. Heat Mass Transfer* **27**, 815–827.

BENJAMIN, G. B. 1957 Wave formation in laminar flow down an inclined plane. *J. Fluid Mech.* **2**, 554–574.

BENNEY, D. J. 1966 Long waves in liquid films. *J. Math. Phys.* **45**, 150–155.

BERBENTE, C. P. & RUCKENSTEIN, E. 1968 Hydrodynamics of wave flow. *AIChE J.* **14**, 772–782.

BUNOV, A. V., DEMEKHIN, YE. A. & SHKADOV, V. YA. 1984 Nonuniqueness of wave solutions in viscous layer. *Prikl. Mekh. i Mat.* **48**, 691–696.

CHANG, H.-C. 1987 Evolution of nonlinear waves on vertically falling films – A normal form analysis. *Chem. Engng Sci.* **42**, 515–533.

CHANG, H.-C. 1989 Onset of nonlinear waves on falling films. *Phys. Fluids* A **1**, 1314–1327.

DEMEKHIN, YE. A., DEMEKHIN, I. A. & SHKADOV, V. YA. 1983 Solitons in flowing layer of a viscous fluid. *Izv. Akad. Nauk. SSSR, Mekh. Zhid. i Gasa* **4**, 9–16.

GESHEV, P. I. & EZDIN, B. S. 1985 Calculation of the velocity profile and that of the wave shape of flowing liquid film. In *Hydrodynamics and Heat-Mass Transfer of the Liquid Flow with Free Surface* (ed. I. R. Shreyber), pp. 49–58. Inst. Thermophysics, Novosibirsk.

GJEVIK, B. 1970 Occurrence of finite-amplitude surface waves on falling liquid films. *Phys. Fluids* **13**, 1918–1925.

KAPITZA, P. L. 1948 Wave flow of thin viscous liquid films. *Zh. Teor. Fiz.* **18**, 3–28.

KAPITZA, P. L. & KAPITZA, S. P. 1949 Wave flow of thin viscous liquid films. *Zh. Teor. Fiz.* **19**, 105–120.

KRANTZ, W. B. & GOREN, S. L. 1971 Stability of thin liquid films flowing down a plane. *Indust. Engng Chem. Fundam.* **10**, 91–101.

LEVICH, V. G. 1959 *Physics-Chemical Hydrodynamics.* Moscow, 699pp.

NAKORYAKOV, V. E., *et al.* 1977 Instantaneous velocity profiles in a wave liquid film. *Inzh. Fiz. J., SSSR* **33**, 399–405.

NAKORYAKOV, V. E., POKUSAEV, B. G. & ALEKSEENKO, S. V. 1981 Desorbtion of weakly-solution gas from flowing liquid films. In *Calculation of Heat and Mass Transfer in Energy-Chemical Processes* (ed. A. P. Burdukov), pp. 23–36. Institute of Thermophysics, Novosibirsk.

NEPOMNYASHCHY, A. A. 1974 Wave regime stability in a film falling down inclined surfaces. *Izv. Akad. Nauk. SSSR, Mekh. Zhid. i Gasa* **3**, 28–34.

NUSSELT, W. 1916 Die oberflachenkondesation des Wasserdampfes. *Teil* I, II. *Z.VDI.* **27**, 541; **28**, 569.

SHKADOV, V. YA. 1967 Wave modes in the gravity flow of a thin layer of a viscious fluid. *Izv. Akad. Nauk. SSSR, Mekh. Zhid. i Gasa* **1**, 43–51.

SHKADOV, V. YA. 1968 On the theory of wave flows of a thin layer of a viscous fluid. *Izv. Akad. Nauk. SSSR, Mekh. Zhid. i Gasa* **3**, 20–25.

SHKADOV, V. YA. 1977 Single waves in the thin layer of a viscous fluid. *Izv. Akad. Nauk. SSSR, Mekh. Zhid. i Gasa* **1**, 63–66.

SIVASHINSKY, G. I. & MICHELSON, O. M. 1980 On irregular wavy flow of a liquid film down a vertical plate. *Prog. Theor. Phys.* **63**, 2112–2114.

TSVELODUB, O. YU. 1980 Stationary running waves on a film falling down inclined surfaces. *Izv. Akad. Nauk. SSSR, Mekh. Zhid. i Gasa* **4**, 142–146.

TSVELODUB, O. YU. & TRIFONOV, YU. YA. 1989 On steady-state travelling solutions of an evolution equation describing the behaviour of disturbances in active dissipative media. *Physica D* **39**, 336–351.

YIH, C.-S. 1963 Stability of liquid flow down an inclined plane. *Phys. Fluids* **6**, 321–335.